Shape optimization and level set method in full waveform inversion with 3D body reconstruction

Zhaohui Guo and Maarten V. de Hoop, Purdue University*

SUMMARY

Full waveform inversion (FWI) in the presence of salt bodies with high wavespeeds as well as sharp and irregular boundaries has been a major challenge in computational seismology. In this paper, we consider the 3D salt body reconstruction problem using a variational formulation of shape optimization. We study the shape functional using the Helmholtz equation and shape derivative to calculate the gradient descent direction for surface boundary deformation. The level set method is employed to represent domains and their boundaries and the dynamic evolution of shape changes. The performance of the approach is demonstrated by a 3D numerical experiment.

INTRODUCTION

We consider an inverse boundary value problem for the Helmholtz equation based on the full waveform modeling. Recently, full waveform inversion (FWI) has received much attention because of the efficiency of the algorithm and high resolution imaging results. Pratt et al. (1998) gave a general formulation of frequency domain FWI involving the computations of forward wave propagation and adjoint problem. FWI is typically implemented using a gradient based iterative method, or a BFGS relevant quasi-Newton method. However recent research shows that the seismic inverse problem is difficult to solve in the presence of salt bodies. Reasons for this include the relatively high wavespeed within salt bodies versus the low wavespeed of the background, and the irregular sharp boundaries. To overcome the difficulty, we consider a variational shape optimization and level set based salt body reconstruction method.

The level set method in inverse problems can be traced back at least to the paper of Santosa (1996) which proposed an approach for general classes of inverse problems involving the reconstruction of obstacle shapes using the level set method. Litman et al. (1998); Dorn et al. (2000); Ramananjaona et al. (2001) further studied this shape optimization method and explored the applications. Burger (2002) developed a functional-analytic framework for construction of the level set method for shape optimization and body reconstruction.

Our shape optimization is a 3D extension work of the paper (Guo and de Hoop, 2012). Based on the same idea, we consider a shape functional based on the solution of the Helmholtz equation and the shape derivative derived from the relevant functions using Lagrange multipliers. We use a velocity method to define the gradient flow of boundary deformation. The gradient descent direction of the boundary deformation is computed by the shape derivative. To demonstrate the feasibility of our approach, a 3D numerical model with salt bodies is presented.

THEORY

We consider a shape functional $\mathscr{J}(\Omega)$ in the following form

$$\mathscr{J}(\Omega) = \mathscr{J}(\Omega, u(\Omega)) = \int_{\Sigma} \varphi(u(\Omega) - d)\mathrm{d}\sigma, \qquad (1)$$

where Ω is the domain to be reconstructed with boundary $\Gamma = \partial\Omega$. Σ is a surface enclosing Ω and φ is a non-negative function inducing a norm. $u(\Omega)$ is a solution of the Helmholtz equation in a configuration containing a subdomain Ω and d is data.

Given a velocity field V, the deformation of domains and boundaries has the form

$$\Gamma_t = \{x_t \mid x \in \Gamma\}, \quad \Omega_t = \{x_t \mid x \in \Omega\}. \qquad (2)$$

where $x_t = x + tV$.

The shape derivatives of functional $\mathscr{J}(\Omega)$ in the velocity field V are given by

$$D\mathscr{J}(\Omega)V = \lim_{t\to 0} \frac{\mathscr{J}(\Omega_t) - \mathscr{J}(\Omega)}{t}. \qquad (3)$$

In general, we can represent the derivative as

$$D\mathscr{J}(\Omega)V = (\rho, v)_{L^2(\Gamma)}, \qquad (4)$$

for some $\rho \in L^2(\Gamma)$, with $v = V \cdot n$ and n denotes the outward normal direction on Γ. Formulation (4) implies that the shape derivative only relies on the normal component of the boundary velocity as the tangential component of velocity field does not induce any change in the shape.

The shape derivative $D\mathscr{J}(\Omega)V$ generates a way to find a descent direction that will maximize the decrease in the functional $\mathscr{J}(\Omega)$. If we can write the shape derivative in the form (4), the standard choice of the gradient flow follows from the inner product $\langle .\ , .\rangle$ in $L^2(\Gamma)$: $V = -\rho n$ on Γ. Then we have

$$D\mathscr{J}(\Omega)V = (\rho, v)_{L^2(\Gamma)} = -(\rho, \rho)_{L^2(\Gamma)} \leq 0. \qquad (5)$$

Level set method

The level set method is a powerful tool to represent a moving interface within a 2D or 3D domain. The method was first introduced by Osher and Sethian (1988), and widely used in the field of image analysis, fluid dynamics and computer vision. The main idea is to formulate the interface as the zero level set of a higher dimensional level set function. The motion of the interfaces can be formulated as the evolution of the level set function $\phi(x(t), t)$, which is Lipschitz continuous, defining

$$\Gamma_t = \{x \mid \phi(x,t) = 0\}, \quad \Omega_t = \{x \mid \phi(x,t) > 0\}. \qquad (6)$$

If the outward normal of the interface Γ_t is n_t, we have

$$n_t(x) = \frac{\nabla\phi(x,t)}{|\nabla\phi(x,t)|}, \quad x \in \Gamma_t.$$

DOI http://dx.doi.org/10.1190/segam2013-1057.1

The time evolution of ϕ is given by a normal velocity $v(x,t)$,

$$\frac{\partial \phi}{\partial t} = -v(x,t)\,|\nabla \phi|. \tag{7}$$

One advantage of the level set method is that it can easily handle topological changes such as splitting and merging of the interfaces. Thus we can allow a flexible geometric and topological representation of the domain Ω.

During the evolution irregularities often develop and in this case it is necessary to re-initialize the level set function (Sussman et al., 1994; Sethian, 1999; Osher and Fedkiw, 2003). The usual method of re-initialization is to find the steady state solution of the equation

$$\frac{\partial \psi}{\partial t} = sign(\phi)\,(1-|\nabla \psi|), \tag{8}$$

where ϕ is the level set function to be re-initialized. The re-initialized level set function $\psi(x,t)$ has the same zero level set Γ_t as $\phi(x,t)$ and gives the signed normal distance to the interface. Note that the property $|\nabla \psi| = 1$ corresponds with the fact that ψ is a signed distance function.

In our computation, instead of performing re-initialization, we employ a penalty term added to the energy functional to maintain the signed distance property as in (Li et al., 2010),

$$\mathscr{R}_p(\phi) = \int_\Theta p(|\nabla \phi|)\,\mathrm{d}x, \tag{9}$$

where the potential function $p(s)$ must be chosen with a minimum at $s=1$ to keep $|\nabla \phi| = 1$. For instance, $p = \frac{1}{2}(s-1)^2$ is preferred with $s=1$ as the unique minimum point.

One major application of the level set method is image segmentation. Here we use it to obtain the initial salt bodies. We assume that the wavespeed model is an image $I(x)$ and introduce segmentation via an edge-based active contour model with a distance regularized level set implementation (DRLSE) (Li et al., 2010). To segment the salt bodies, we start with an initial level set function with the zero level set that is a closed curve or surface around the salt bodies, then evolve to identify the boundaries of the salt bodies. The energy functional takes the form

$$\mathscr{E}(\Omega) = \int_\Theta p(|\nabla \phi|)\,\mathrm{d}x + \gamma \int_\Theta g\delta(\phi)|\nabla \phi|\,\mathrm{d}x + \mu \int_\Theta gH(\phi)\,\mathrm{d}x. \tag{10}$$

where p is defined as in the previous paragraph to keep the signed distance property, δ and H denote the Dirac measure and the Heaviside function, γ and μ are weighting parameters, and g is an edge detector function which takes on small values near boundaries. For example

$$g = \frac{1}{1+\beta|\nabla I|^2}. \tag{11}$$

The energy functional (10) works as an edge detector to locate the final boundary at the points of maximum $|\nabla I(x)|$, and can be minimized by solving the following gradient flow equation:

$$\begin{aligned} \frac{\partial \phi}{\partial t} &= \nabla \cdot \left(p'(|\nabla \phi|)\frac{\nabla \phi}{|\nabla \phi|} \right) + g\delta(\phi)\left(\gamma \nabla \cdot \frac{\nabla \phi}{|\nabla \phi|} - \mu \right) \\ &= \left(\nabla^2 \phi - \nabla \cdot \frac{\nabla \phi}{|\nabla \phi|} \right) + g\delta(\phi)\left(\gamma \nabla \cdot \frac{\nabla \phi}{|\nabla \phi|} - \mu \right). \end{aligned}$$

THE SHAPE DERIVATIVE BASED ON HELMHOLTZ EQUATION

We denote a bounded domain Θ and an open connected domain D with $\Omega \subset D \subset \Theta$. Let Σ be an open portion of ∂D, and suppose $supp(f) \subseteq \Theta \backslash \overline{D}$. We denote $q(x) = \omega^2 c^{-2}(x)$ and the wavefield u takes u^+ and u^- as the limit from the exterior and interior of Γ. $f \in H^{-1}(\Theta)$ represents a volume source. Then we consider a partitioned boundary value problem as in (Carpio and Rapún, 2008)

$$\left\{ \begin{array}{rcll} (-\Delta - q_2(x))u &=& f, \quad x \in \Theta \backslash \overline{\Omega} & , \\ (-\Delta - q_1(x))u &=& 0, \quad x \in \Omega & , \\ u^- - u^+ &=& 0, \quad x \in \Gamma & , \\ \dfrac{\partial u^-}{\partial \nu} - \dfrac{\partial u^+}{\partial \nu} &=& 0, \quad x \in \Gamma & , \\ \dfrac{\partial u}{\partial \nu} &=& -\Lambda_e u, \quad x \in \partial\Theta & , \end{array} \right. \tag{12}$$

where Λ_e is the exterior Dirichlet-to-Neumann map for the Helmholtz equation on Θ'.

We introduce the shape functional based on solution of Helmholtz equation $u_t = S(\Omega_t; q_1, q_2)f$

$$\mathscr{J}(\Omega_t, q_1, q_2) = \frac{1}{2}\|P(S(\Omega_t; q_1, q_2)f - d_f)\|^2_{L^2(\Sigma)}. \tag{13}$$

Here, d_f represents the data, P is an elliptic operator such that $\|Pd\|_{L^2(\Sigma)} = \|d\|_{H^{3/2}(\Sigma)}$. Taking the derivative with respect to t yields

$$\begin{aligned} &\frac{\mathrm{d}}{\mathrm{d}t}\mathscr{J}(\Omega_t, q_1, q_2)\mid_{t=0} = \\ &Re \int_\Sigma [P^* P(S(\Omega_t; q_1, q_2)f - d_f)]\ \frac{\mathrm{d}}{\mathrm{d}t} S(\Omega_t; q_1, q_2)f \mid_{t=0} \mathrm{d}\sigma. \end{aligned}$$

To get an expression for the shape derivative we introduce a Lagrange multiplier w and a family of functionals

$$\begin{aligned} \mathscr{L}(\Omega_t; v, w) &= \mathscr{J}(\Omega_t, q_1, q_2) + Re\,(b(\Omega_t; v, w) - s(w)) \\ &= \frac{1}{2}\|P(v - d_f)\|^2_{L^2(\Sigma)} + Re\,(b(\Omega_t; v, w) - s(w)) \end{aligned}$$

where $b(\Omega; v, w)$ and $s(w)$ come from the variational equation of (12)

$$b(\Omega; u, v) = s(v) \quad for\ all\ v \in H^1(\Theta), \tag{14}$$

where

$$b(\Omega; u, v) = \int_{\Theta \backslash \overline{\Omega}} (\nabla u \cdot \nabla \bar{v} - q_2 u \bar{v})\,\mathrm{d}x + \int_\Omega (\nabla u \cdot \nabla \bar{v} - q_1 u \bar{v})\,\mathrm{d}x$$

and

$$s(v) = \int_{\Theta \backslash \overline{D}} f\,\bar{v}\,\mathrm{d}x - \int_{\partial\Theta} (\Lambda_e u)\,\bar{v}\,\mathrm{d}\sigma.$$

Using an augmented Lagrangian method and employing the adjoint state method, as in the paper (Guo and de Hoop, 2012), we obtain

$$D\mathscr{J}(\Omega, q_1, q_2)V = Re\,\{ \int_\Gamma (q_1 - q_2)\,u\bar{w}\,\vec{n} \cdot V\,\mathrm{d}\sigma \,\} = \int_\Gamma \rho v\,\mathrm{d}\sigma, \tag{15}$$

DOI http://dx.doi.org/10.1190/segam2013-1057.1

where $\bar{w} \in H^1(\Theta)$ is the solution of the adjoint equations

$$\begin{cases} (-\Delta - q_2(x))\bar{w} &= [P^* P(S(\Omega_t; q_1, q_2) f - d_f)]\, \delta_\Sigma, \quad w \in \Theta \backslash \overline{\Omega} \\ (-\Delta - q_1(x))\bar{w} &= 0, \quad w \in \Omega \\ \bar{w}^- - \bar{w}^+ &= 0, \quad w \in \Gamma \\ \dfrac{\partial \bar{w}^-}{\partial \nu} - \dfrac{\partial \bar{w}^+}{\partial \nu} &= 0, \quad w \in \Gamma \\ \dfrac{\partial \bar{w}}{\partial \nu} &= -\Lambda_e \bar{w}, \quad w \in \partial\Theta \end{cases} \tag{16}$$

We have made use of the fact that $\Lambda_e^*(\bar{w}) = \overline{\Lambda_e w}$, and w^+, w^- are defined in the same way as u^+, u^-.

Given the shape derivative, we can generate the corresponding gradient flow based on the level set function

$$\begin{aligned} \frac{\partial \phi}{\partial t} &= -v(x,t)\,|\nabla \phi|, \\ &= Re\{(q_1(x) - q_2(x))\, u(x,t) \bar{w}(x,t)\}\,|\nabla \phi|. \end{aligned}$$

In practice, the narrowband method is implemented with DRLSE formulation (9)

$$\mathscr{R}_p(\phi) = \int_\Theta \frac{1}{2}(|\nabla \phi - 1)^2 \, dx.$$

The final evolution is then given by

$$\begin{aligned} \frac{\partial \phi}{\partial t} &= \left(\nabla^2 \phi - \nabla \cdot \frac{\nabla \phi}{|\nabla \phi|} \right) \\ &+ Re\{(q_1(x) - q_2(x))\, u(x,t) \bar{w}(x,t)\}\,|\nabla \phi|. \end{aligned}$$

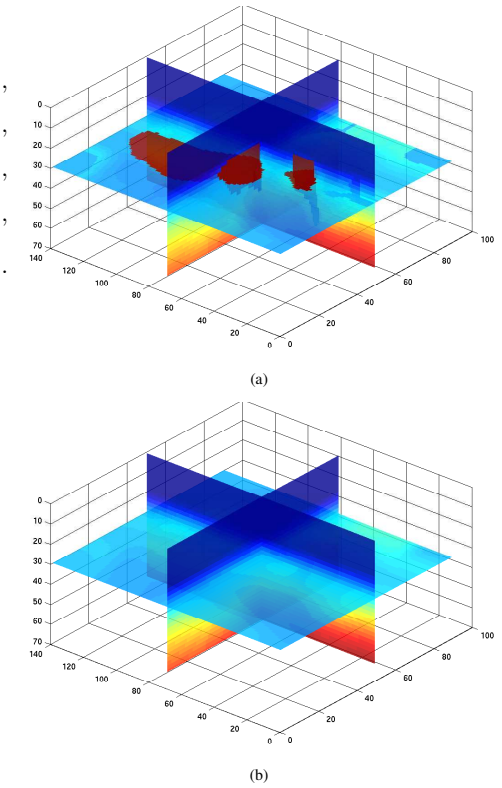

Figure 1: (a): The true 3D modified Louro model; (b): the starting wavespeed model for FWI.

NUMERICAL EXPERIMENTS

We use a 3D modified Louro model to demonstrate our approach. The true wavespeed model is displayed in Figure 1(a) and contains two salt bodies. The wavespeed varies from 1500 m/s to 4500 m/s. The model is discretized onto a 140x90x62 mesh grid with uniform step sizes $hx = hy = hz = 20m$. We consider 21x15 shot sources and 45x41 receivers evenly distributed on the top surface. To obtain the initial guess of salt bodies, we use a starting model to perform FWI as in Figure 1(b), which does not contain any information about the salt. We choose five frequencies (2.0, 4.0, 5.7, 8.0, 10.0)Hz with 10 iterations per frequency. The result is presented in Figure 2.

We then perform the level set segmentation to estimate the shape of the salt bodies. To better visualize the 3D level set function, we use the isosurface of zero level set to present the salt bodies. Figure 3(a) presents the segmented salt bodies from the resulting inverted wavespeed model, which is used as the initial shape Ω_0 in the shape optimization procedure. Figure 3(b) presents the true salt bodies segmented from the true wavespeed model.

We employ the iterative level set evolution method with descent direction deduced from the shape derivative. The salt body reconstructions are displayed in Figures 4(a)-(d). We note the significant improvement of the salt bodies by shape optimization. It can also be noted that the resulting salt bodies agree very well at the top boundaries, but not at the bottom. Since data is only measured at the top surface, we have to expect a better reconstruction of the top boundary than the bottom boundary.

CONCLUSION

In this paper, we presented the application of 3D shape optimization and the level set method to the seismic inverse problem and salt body reconstruction. We made use of a level set function to construct the boundaries and formulate the evolution. We also computed shape derivatives to obtain the gradient flow for the boundary evolution and recover the salt boundaries. A numerical example of a 3D Louro model shows the feasibility of this reconstruction method.

ACKNOWLEDGMENTS

This work is partially supported by the National Science Foundation under grant CMG-1025259 and partially by the members of the Geo-Mathematical Imaging Group at Purdue University. We also think Total for providing the 3D Louro model.

DOI http://dx.doi.org/10.1190/segam2013-1057.1

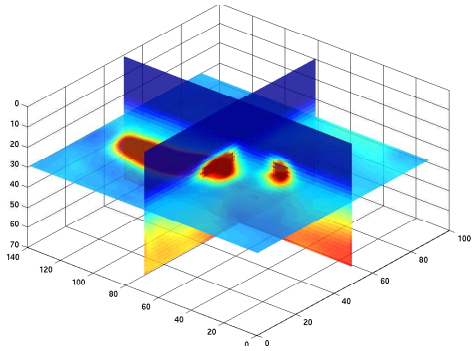

Figure 2: The FWI inverted wavespeed model.

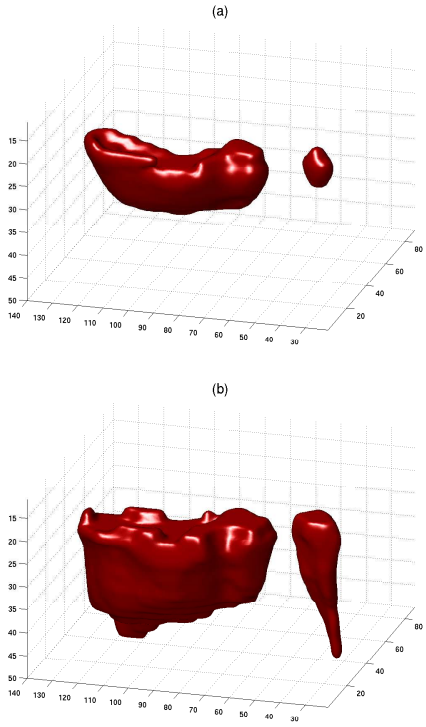

Figure 3: (a): Initial salt body for shape optimization; (b): the true salt body.

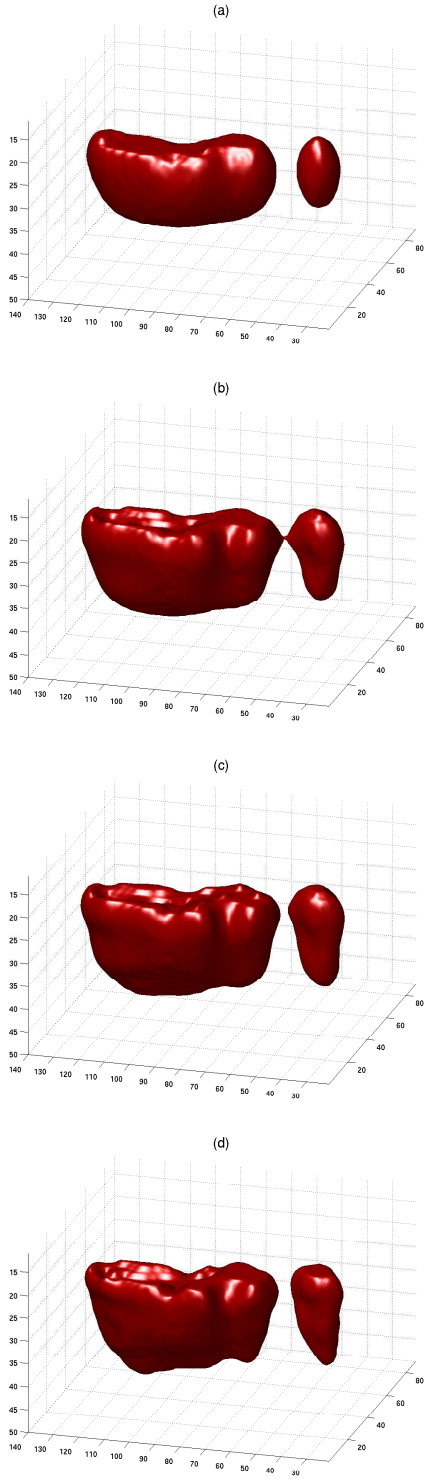

Figure 4: (a)-(d) the evolved salt bodies in the shape optimization iterations.

DOI http://dx.doi.org/10.1190/segam2013-1057.1

http://dx.doi.org/10.1190/segam2013-1057.1

EDITED REFERENCES

Note: This reference list is a copy-edited version of the reference list submitted by the author. Reference lists for the 2013 SEG Technical Program Expanded Abstracts have been copy edited so that references provided with the online metadata for each paper will achieve a high degree of linking to cited sources that appear on the Web.

REFERENCES

Burger, M., 2002, A framework for the construction of level set methods for shape optimization and reconstruction: Interfaces and Free Boundaries, **5**, 301–329.

Carpio, A., and M.-L. Rapun, 2008, Solving inhomogeneous inverse problems by topological derivative methods: Inverse Problems, **24**, 045014.

Dorn, O., E. Miller, and C. Rappaport, 2000, A shape reconstruction method for electromagnetic tomography using adjoint fields and level sets: Inverse Problems, **16**, 1119–1156.

Guo, Z., and M. de Hoop, 2012, Shape optimization in seismic inverse problems with sparse blocky model representations: Geo-Mathematical Imaging Group (GMIG) Project Review.

Li, C., C. Xu, C. Gui, and M. D. Fox, 2010, Distance regularized level set evolution and its application to image segmentation: IEEE Transactions on Image Processing, **19**, no. 12, 3243–3254. PubMed

Litman, A., D. Lesselier, and F. Santosa, 1998, Reconstruction of a two-dimensional binary obstacle by controlled evolution of a level-set: Inverse Problems, **14**, 685–706.

Osher, S., and R. Fedkiw, 2003, Level set methods and dynamic implicit surfaces: Springer.

Osher, S., and J. Sethian, 1988, Fronts propagating with curvature-dependent speed: Algorithms based on Hamilton-Jacobi formulations: Journal of Computational Physics, **70**, 12–49.

Pratt, R., C. Shin, and G. Hicks, 1998, Gauss-Newton and full Newton methods in frequency-space seismic waveform inversion: Geophysical Journal International, **133**, 341–362.

Ramananjaona, C., M. Lambert, D. Lesselier, and J. Zolesio, 2001, Digital-image based elastotomography: nonlinear mechanical property reconstruction of homogeneous gelatine phantoms: University of Cambridge.

Santosa, F., 1996, A level-set approach for inverse problems involving obstacles: Control, Optimization Calculus Variation, **1**, 17–33.

Sethian, J., 1999, Level set methods and fast marching methods: Evolving interfaces in computational geometry, fluid mechanics, computer vision, and materials science: Cambridge University Press.

Sussman, M., P. Smereka, and S. Osher, 1994, A level set approach for computing solutions to incompressible two-phase flow: Journal of Computational Physics, **114**, 146–159.